

## Research article

Hygin Davidson Mayekol Mayck\*, Ahmed Mohamed Rashad Fath El-Bab, Evan Murimi and Pierre Moukala Mpele

# A human heartbeat frequencies based 2-DOF piezoelectric energy harvester for pacemaker application

<https://doi.org/10.1515/ehs-2021-0011>

Received June 27, 2021; accepted August 8, 2021;

published online September 6, 2021

**Abstract:** In the last decade, piezoelectric energy harvesters have received a significant attention from the scientific community. This comes along with the need of developing self-powered devices such as medical implant to reduce the cost and risk of surgery. This paper investigates a two degree of freedom (2-DOF) piezoelectric energy harvester device to be integrated into a pacemaker. The 2-DOF is designed as a cut-out beam with a secondary beam cut into a primary one. The system is developed to operate in the frequency range of 0–2 Hz, with an acceleration of 1 g ( $9.8 \text{ m/s}^2$ ) to match the heartbeat frequencies (1–1.67 Hz). The system uses a Lead Zirconate Titanate (PZT) and a Poly Methyl Methacrylate (PMMA) as lead beam to compensate the brittleness of PZT. COMSOL Multiphysics software is used to model and analyze the resonant frequencies of the system, and the stress in the piezoelectric beam. The proposed device has a compact volume of  $26 \times 11.58 \times 0.41 \text{ mm}$ , which can fit perfectly in a pacemaker whose battery volume has been reduced by 50%. The output voltage and power are determined through analytical calculus using Matlab. Typical pacemakers require 1  $\mu\text{W}$  to operate. Thus, with a

peak power of 30.97  $\mu\text{W}$  at 1.5 Hz and an average output power of 11.05  $\mu\text{W}$  observed from 0.9 to 1.7 Hz, the harvester can power a pacemaker. It is assumed that the energy harvester could extend its life time for 5–10 more years. Furthermore, the harvester operates at extremely low frequency and produces reasonable power, making it suitable for biomedical devices.

**Keywords:** 2-DOF; human heartbeat frequencies; pacemaker; piezoelectric energy harvesting.

## Introduction

Harvesting energy consists in collecting the available ambient energy and transforming it into electrical energy to power other devices. The power produced is in the order of micro to milli-Watts, which makes it suitable for low power electronics (Kazmierski and Beeby 2014). Among the forms of energy found in the nature, the mechanical energy is the most present and has an advantage over the thermal and photonic energy as it can be used where these two are not efficient (Beeby and White 2010). Any source of vibration can constitute a source of mechanical energy. The amount of vibration are different from one source to another. Human related vibration are relatively low, less than 10 Hz for human motion (Kazmierski and Beeby 2014) and less than 2 Hz for human heartbeats (Kuan 2017).

The mechanical energy can be transformed into electrical energy using either piezoelectric, electromagnetic or electrostatic transduction techniques (Zhu and Beeby 2011). Electrostatic transduction produces high voltages and is appropriate for micro electromechanic systems (MEMS), but requires an external voltage source to operate (Roundy 2003). On the other hand, electromagnetic transduction is not suitable for medical implant, and its power density is low (Soliman 2009). However, piezoelectric harvesters, mostly cantilever beam, have simple configuration and high conversion efficiency. This makes piezoelectric materials the most popular throughout the research field (Liu et al. 2011a).

**\*Corresponding author: Hygin Davidson Mayekol Mayck**, Department of Mechatronic Engineering, Pan African University Institute of Basic Sciences Technology and Innovation, Nairobi, Kenya, E-mail: davidsonmayck96@gmail.com. <https://orcid.org/0000-0001-5602-6945>

**Ahmed Mohamed Rashad Fath El-Bab**, Department of Mechatronics and Robotics, Egypt-Japan University of Science and Technology, New Borg El-Arab, Alexandria, Egypt

**Evan Murimi**, Department of Mechatronic Engineering, Jomo Kenyatta University of Agriculture and Technology, Nairobi, Kenya

**Pierre Moukala Mpele**, Department of Electrical Engineering, Pan African University Institute of Basic Sciences Technology and Innovation, Nairobi, Kenya, E-mail: pm.mpele@gmail.com. <https://orcid.org/0000-0003-3361-2006>

Piezoelectric materials include inorganic, organic, and composite materials. Inorganic materials such as piezoceramics have high energy conversion, but are very brittle. However, organic materials have low energy conversion but are highly flexible (Bischur and Schwesinger 2012; Nia, Zawawi, and Singh 2017; Sezer and Koç 2020). Polyvinylidene fluoride (PVDF) and PZT are organic and inorganic, respectively, which have been mostly investigated. In a comparative study conducted in (Zhu and Beeby 2011), for generators with the same dimensions, generators using PZT materials have the highest output power over PVDF and barium titanate ( $\text{BaTiO}_3$ ). To compensate the lack of flexibility of inorganic material, and the low power production of organic material, composite piezoelectric materials are developed (Sezer and Koç 2020). This composite material are highly stretchable, some can stretch up to 100% strain (Mokhtari et al. 2021), or have a biaxial stretch of 300% (Zhou et al. 2020). Composite piezoelectric materials are also improved in terms of output voltage (Xu et al. 2020). This create more interest in developing composite piezoelectric materials.

Piezoelectric generators can use human body induced energies to power medical implants or portable electronics, making energy harvesting a promising solution in the development of autonomous system. This include *in vivo* energies, such as heartbeat (Xu et al. 2020) or blood flow (Abdelmageed, El-Bab, and Abouelsoud 2019; Abdelmageed, Fathelbab, and Abouelsoud 2019), and physical activities such as walking, running and handshake (Andanje, Ikua, and Elbab 2019; Ju et al. 2013; Wang et al. 2021). A pacemaker is a medical implant used to regulate the heartbeat. Most of those devices' battery lasts from 5 to 10 years, which make a patient to have several surgeries to replace the battery. Therefore, it is important to develop a system that can charge or power the pacemaker, to increase its live spam. To date, there are two type of pacemakers. The first one is placed outside of the heart and uses lead to sense and regulate the heartbeats, whereas the other one is lead-less and placed directly inside the heart (Medtronic 2020). Typical pacemakers have a power consumption range from few  $\mu\text{W}$  to 20  $\mu\text{W}$  (Mitcheson et al. 2008). The size of a typical lead-pacemaker is about  $42 \times 51 \times 6$  mm, and the battery takes around 2/3 of that volume. The power area can be reduce by 50% to set the maximum size of a vibrational energy harvester as  $27 \times 27 \times 6$  mm (Amin Karami and Inman 2012). However, the lead-less type is 93% smaller than the previous type and requires a minimum of 1.5 V to operate (Medtronic 2017). The size required for an integrated energy harvester is of about 0.3  $\text{cm}^3$  (Colin, Basrour, and Rufer 2013).

The fact that most vibration-based energy harvesters are resonant systems constitute the major challenge of these devices. The maximum power is observed when the resonant frequency of the system matches the excitation frequency, like in the case of an SDOF system. Power generated drops drastically at any other frequency (Zhu and Beeby 2011). To improve the aspect of the harvester, there are techniques of widening the operating frequency, multidirectional harvesting, and non-resonant approach (Maamer et al. 2019). A 2-DOF system is a type of multimodal systems used to improve the performance of harvesters by widening their operational frequency. The harvester has different vibration modes with different resonant frequencies by using more than one seismic mass (Maamer et al. 2019). One 2-DOF beam configuration that is suitable for micro application is the cut-out beam. This configuration is compact and offer a minimum use of the harvester's volume, thus a better power density (Andanje, Ikua, and Elbab 2019; Magdy, El-Bab, and Assal 2014).

Human body related harvesters could be classified into two groups. Wearable harvesters impeded into a portable device, and implanted harvester fixed on internal organs. Some tens of micro and milli Watts were harvested during human activities such as handshaking, walking and slow running (Ju et al. 2013; Wang et al. 2021). Although, the operating frequencies of the devices are low (from 2 to 6 Hz), they might not perform well below 2 Hz. Also the devices are placed either on the arm or the leg of a human being, which inquires a lead connection with a pacemaker placed near the heart. Mostafa et al. developed an SDOF PZT harvester placed inside the Superior Vena Cava (SVC) that aimed to power a pacemaker using the harmonic blood flow forces in (Abdelmageed, El-Bab, and Abouelsoud 2019) for the first scenario, and the blood pressure fluctuation in (Abdelmageed, Fathelbab, and Abouelsoud 2019) for the second scenario. The simulation results were 9 and 3.5  $\mu\text{W}$  for the first and second scenario, respectively. The fact that the devices' geometric parameters are chosen to avoid Superior Vena Cava Syndrome (SVCS) should not mean they are totally risk free. Xu et al. used a single beam around the pacemaker lead to harvest energy from the complex motion of the lead driven by the heartbeats (Xu et al. 2020). However this approach increase the total diameter of the lead and could cause complication during surgery. Some piezoelectric harvester operating at extremely low frequency generates high output power, but with large dimensions, which makes it less appropriate for small devices applications (Wu et al. 2018). Although, it is possible to find a

micro electromechanical system (MEMS) that vibrate at an extremely low frequency of 1.2 Hz with an acceleration of 0.9 g, and provide a maximum electrical power density of  $26.1 \text{ mW/cm}^3$ , the MEMS device does not cover the entire range of heartbeat frequencies (Alrashdan 2020).

The power produced by piezoelectric beam harvesters drops with the size and the operating frequency. Actual pacemakers have limited operational time. There are limited researches in human heartbeat frequencies based energy harvesters for pacemaker application. The challenges in this area are the size and frequency requirements. This paper aims to develop an energy harvester that can be used to power a pacemaker, and hence extend its operational time. The energy harvester is to be integrated directly inside the pacemaker. The present work minimizes the size of the harvester, matches the heartbeat frequencies, and meet the requirement for powering pacemakers. The proposed device use a flexible PMMA lead beam to compensate the brittleness of PZT, and has shown the ability to operate at extremely low frequencies.

## Design of the harvester

The system is designed to match the heartbeat frequencies from 1 to 1.67 Hz (Kuan 2017), and its dimensions have to respect a strict volume of  $27 \times 27 \times 6 \text{ mm}$  (Amin Karami and Inman 2012). The harvester is designed with PMMA as lead beam, and the piezoelectric beam (PZT-5A) is placed on the top flat face of the beam. The tip mass is made of copper with a density of  $8960 \text{ kg/m}^3$ . A beam build with only PZT would produce higher output power and voltage, but would be much longer and could exceed the maximum length of 27 mm. The PMMA has a Young's Modulus of 3.2 GPa and a maximum allowed stress of 10.4 MPa (Kaysons). The parameters of PZT used are shown in Table 1.

The resonant frequency of a beam depends directly on its geometric parameters, but is most sensitive to change in thickness (Panchenko et al. 2020). However, there is a direct relationship between the resonant frequency and the

stress in the beam. Considering an SDOF beam with a lead and piezoelectric beams having the same dimensions, different geometric combinations of length (25 and 26 mm), width (1–5 mm) and thickness (4–10  $\mu\text{m}$ ) shows that the stress decreases as the resonant frequency increases. The results of eigenfrequencies and stress simulation run on COMSOL Multiphysics, support the previous affirmation (Figure 1). In Figure 1(a) and (b), the length and width do not have a big influence on the stress and frequency variation, while Figure 1(a) shows clearly that the frequency increases with the thickness, when the stress reduces. However in Figure 1(b), a width of 1–2 mm produces a relatively low frequency. To reduce the resonant frequency and ensure an acceptable stress (below 10 MPa), the length and thickness of the piezoelectric beam can be reduced, while those of the lead beam are kept to the maximum, and a tip mass can be added.

The total length of the harvester is here chosen to be less than 27 mm. This is to allow the harvester to fit into the pacemaker, and have a margin of oscillation. Figure 2 illustrates the beam dimensions and shows how it can fit in the available space in a pacemaker.  $k_1/2$  represents half of the primary beam, while  $k_2$  represents the secondary beam. One piezoelectric beam is placed on the secondary beam, while two of them are placed on the primary beam.

## Operational principle

The energy harvester is designed using the concept of the classic undamped dynamic absorber (Den Hartog 1985). The system has two different natural frequencies, two springs and two masses. One main mass for the primary beam and an absorber mass for the secondary beam, as shown in Figure 3.

The 2-DOF harvester is designed as a cut out beam. Hence the system in Figure 2 can be represented as in Figure 4(a), composed by an outer beam with a stiffness  $k_1$  and mass  $m_1$ , and an inner beam with a stiffness  $k_2$  and mass  $m_2$ . The difference between the cut out beam and the classical undamped dynamic absorber is that the main stiffness  $k_1$  is divided into two, but the dynamic equation of the systems are the same (Equation (1)) (Magdy et al. 2014).

$$\begin{bmatrix} m_1 & 0 \\ 0 & m_2 \end{bmatrix} \begin{bmatrix} \ddot{x}_1 \\ \ddot{x}_2 \end{bmatrix} + \begin{bmatrix} k_1 + k_2 & -k_2 \\ -k_2 & k_2 \end{bmatrix} \begin{bmatrix} x_1 \\ x_2 \end{bmatrix} = \begin{bmatrix} F \\ 0 \end{bmatrix} \quad (1)$$

where  $F = f_o \sin(\omega t)$  is the harmonic excitation force,  $f_o$  and  $\omega$  are respectively its the amplitude and frequency. The displacement of  $m_1$  and  $m_2$  are respectively  $x_1$  and  $x_2$ . The amplitudes  $X_1$  and  $X_2$  are expressed as:

**Table 1:** Piezoelectric materials properties (Gusarov 2015; Rob Carter 2021).

Properties	Units	PZT-5A
Young's modulus ( $Y$ )	GPa	54
Tensile strength	MPa	20
Strain coefficient ( $d_{31}$ )	$10^{-12} \text{ m/v}$	−190
Coupling coefficient ( $k_{31}$ )	%	35
Dielectric constant ( $K^T$ )		1800

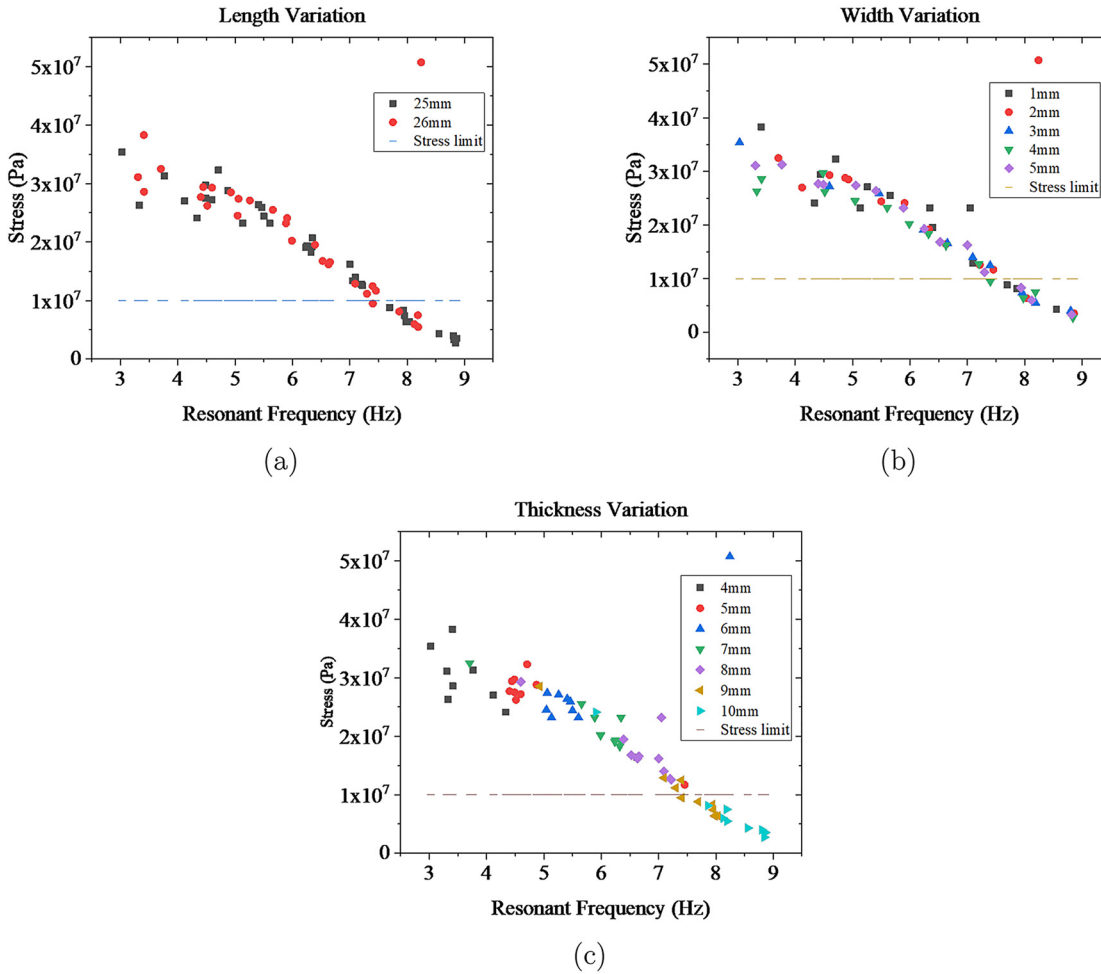


**Figure 1:** Resonant frequency versus stress: (a) Length variation; (b) width variation; (c) thickness variation.

$$X_1 = \frac{(k_2 - m_2 \omega^2) f_0}{(k_1 + k_2 - m_1 \omega^2)(k_2 - m_2 \omega^2) - k_2^2} \quad (2)$$

$$X_1 = \frac{k_2 f_0}{(k_1 + k_2 - m_1 \omega^2)(k_2 - m_2 \omega^2) - k_2^2} \quad (3)$$

From Equation (2), the amplitude  $X_1$  of the mass  $m_1$  becomes zero when the excitation frequency is equal to  $\omega_{22} = \sqrt{k_2/m_2}$ . The amplitude of  $m_2$  becomes  $X_2 = -f_0/k_2$  as shown in Figure 4(b). This is the condition for the secondary system to operate as a vibration absorber, suppressing the displacement of the first mass. The maximum power that can be gained from a 2-DOF harvester system, is the amount of dissipated energy by the damping ratio ( $c$ ) due to transduction from mechanical to electrical energy (Magdy, El-Bab, and Assal 2014). Both the primary and secondary beam generate power depending on their amplitude.

For the primary beam:

$$P = c \omega^2 (X - X_1)^2 \quad (4)$$

For the secondary beam:

$$P = c \omega^2 (X_2 - X_1)^2 \quad (5)$$

$X$  is the amplitude of the input signal and is equal to the ratio of the input acceleration ( $a$ ) by the input frequency (Equation (6)). The input acceleration is equal to 1 g ( $9.8 \text{ m/s}^2$ ).

$$X = -a/\omega \quad (6)$$

## System parameters' selection

The design process is illustrated in Figure 5. To allow the system to operate in the human heartbeat frequency range,

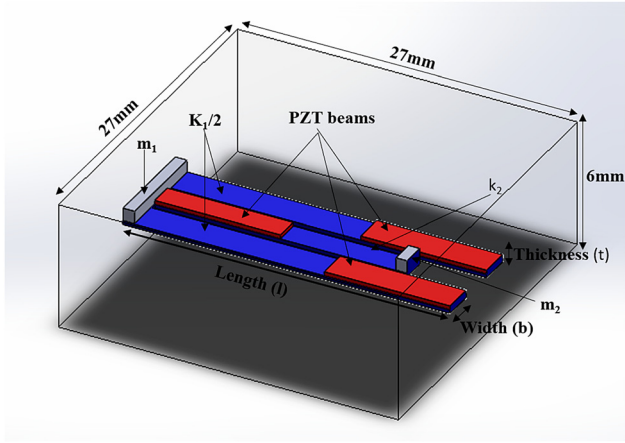


Figure 2: System illustration.

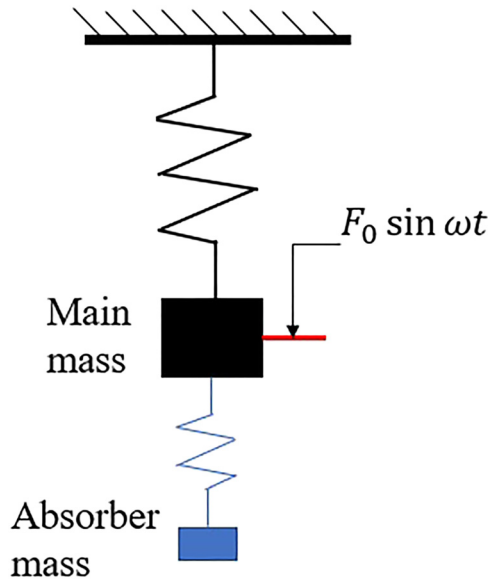


Figure 3: The classical undamped tuned dynamic absorber.

the main frequency  $\omega_{22}$  is chosen equal to 1.3 Hz, which is approximately the middle of the frequency range. Considering a bandwidth of  $\pm 20\%$  from the main frequency, the two modal frequencies are set at  $\omega_1 = 1.04$  Hz and  $\omega_2 = 1.54$  Hz.

The length of the primary beam is first chosen to be 26 mm, for the system to fit in the available volume of  $27 \times 27 \times 6$  mm. The dimensions of the secondary beam are set accordingly to the simulation results shown in Figure 1. The thickness of the secondary beam is chosen to be  $10 \mu\text{m}$ , and its width 2 mm. Its length is determined in respect of the relation  $2l_2 \neq 3l_1$  (from 18 to 24 mm) to avoid the system to operate like to separate beam (Zayed et al. 2019). The stiffness is determined using Equation (7). At a micro scale, the stiffness  $k_2$  of the secondary beam is the equivalent

stiffness of the driving beam and the piezoelectric beam mounted in series. This equivalent stiffness is determined using Equation (8).

$$k = \frac{3EI}{l^3} \quad (7)$$

$$k_{eq} = \frac{1}{\frac{1}{k_p} + \frac{1}{k_b}} \quad (8)$$

where  $E$  is the young modulus of the beam, and  $I = (bt^3)/12$  is the moment of inertia of the beam.  $k_{eq}$  is the equivalent stiffness and  $k_p$  and  $k_b$  are respectively the stiffness of the piezoelectric and driving beam. The value of stiffness obtained helps to determine the tip mass  $m_2$  (or proof mass) using Equation (9). The proof mass is considered to be the mass of the system because the mass of the beam is negligible compared to it (Renaud et al. 2009).

$$m = \frac{k}{\omega^2} \quad (9)$$

Once the mass is obtained, the stress  $\sigma$  is determined using Equation (10), and compare with the maximum allowed stress in the lead beam. If the stress is above 10 MPa, the dimension of the secondary beam can be modified, then the stiffness  $k_2$  and mass  $m_2$  are recalculated. If the stress is below 10 MPa, the next step is to calculate the stiffness  $k_1$  and tip mass  $m_1$  of the primary beam.

$$\sigma = \frac{6mal}{bt^2} \quad (10)$$

where  $m$ ,  $a$ ,  $l$ ,  $b$  and  $t$  are respectively the tip mass, the input acceleration ( $9.8 \text{ m/s}^2$ ), the length, width and thickness of the beam.

The relationship between the two resonant frequencies  $\omega_1$  and  $\omega_2$ , and the system parameters,  $m_1$ ,  $m_2$ ,  $k_1$  and  $k_2$ , is obtained from the dynamic equation of the system (Thomson 1996). The mass and stiffness of the primary beam can then be determined using Equations (11) and (12) (Magdy et al. 2014).

$$\omega_1^2 \times \omega_2^2 = \frac{k_1}{m_1} \times \frac{k_2}{m_2} \quad (11)$$

$$\omega_1^2 + \omega_2^2 = \frac{k_1}{m_1} + \frac{k_2}{m_2} + \frac{k_2}{m_1} \quad (12)$$

where  $\omega_1$  and  $\omega_2$  are respectively equal to  $\omega - 20\%$  and  $\omega + 20\%$ ,  $k_1$  and  $m_1$  are the stiffness and mass of the primary beam respectively.

The thickness of the primary beam is equal to the one of the secondary beam. The width corresponding to  $k_1/2$  is needed to build the system, and can be obtained using Equation (13)

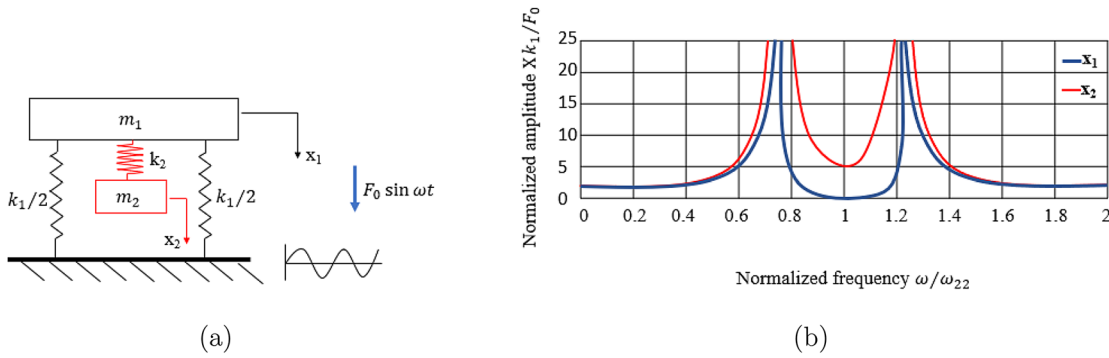


**Figure 4:** Absorber model: (a) schematic diagram of the vibration absorber with cut-out design; (b) normalized amplitude versus normalized frequency.

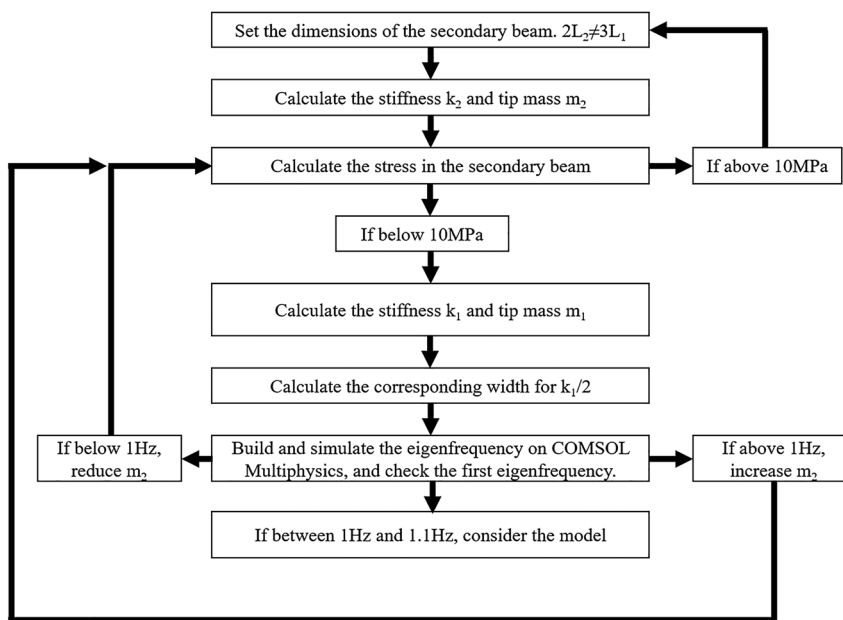


**Figure 5:** System parameters' selection process.

$$b_{k_1/2} = \frac{2l_1 k_1}{Et_1^3} \quad (13)$$

The width and length of the primary beam is superior to those of the secondary beam, the stress in the first beam is smaller than the one in the second. Once all the system's parameters are known, the system is built on COMSOL Multiphysics, where the eigenfrequency simulation is run. If the first frequency is below 1 Hz, the mass  $m_2$  is reduced, while the mass is increased if superior to 1 Hz.

## Voltage and power output

An illustration of the electrical circuit of the piezoelectric generator is shown in Figure 6.  $CR_s R_L$  and  $V_{oc}$  are the capacitance between two electrodes, the internal resistance,

the load resistance and the open-circuit voltage, respectively. According to Liu et al. (Liu et al. 2011b), the open circuit voltage generated by a beam with a piezoelectric layer deposited on top is a function of the piezoelectric material properties and the strain distribution along the beam top surface.

$$\xi(x) = \frac{3t_b}{l_b} \left( \frac{2l_b + l + m - 2x}{4l_b^2 + 9l_b l_m + 6l_m^2} \right) \sigma_m \quad (14)$$

$$V_{oc} = \frac{-d_{31} Y t_c}{\epsilon_{33} l_b} \int_0^{l_b} \xi(x) dx \quad (15)$$

$$V_{oc} = -\frac{d_{31} Y t_c}{\epsilon_{33} l_b} \frac{(l_b + l_m) t_b \delta_m}{4l_b^2 + 9l_b l_m + 6l_m^2} \quad (16)$$

where  $V_{oc}$  is the open circuit voltage,  $Y$  is the Young's modulus of the piezoelectric material,  $d_{31}$  is the transverse-axial

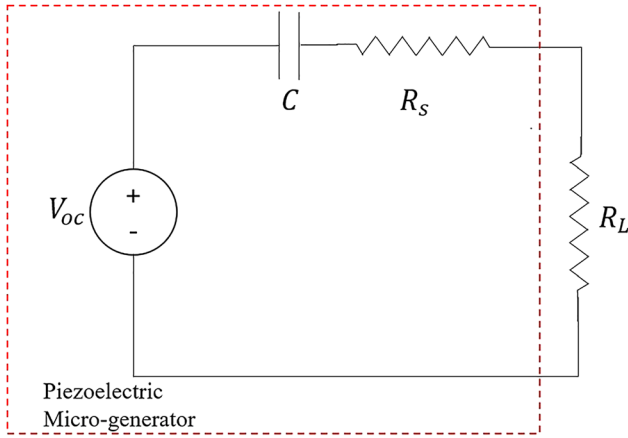


Figure 6: Electrical circuit of a piezoelectric generator.

piezoelectric constant,  $\epsilon_{33}$  is the transverse dielectric coefficient,  $t_c$  and  $t_b$  are respectively the thickness of the piezoelectric layer and beam,  $l_m$  and  $l_b$  are the length of the tip mass and the beam respectively,  $\sigma_m$  is the displacement of the tip mass and  $\xi(x)$  is the strain distribution. The transverse dielectric constant is the product of the dielectric constant with the permittivity of piezoelectric material to the empty space ( $\epsilon_0 = 8.854 \times 10^{-12} \text{F/m}$ ) (Rob Carter 2021).

The internal resistance of the piezoelectric material is very low, close to zero (Zhu and Beeby 2011). The piezoelectric impedance  $Z_p$  is then only the one of the capacitance  $C$ , which is determined using Equation (18) (Rob Carter 2021).

$$C = \frac{K^T \epsilon_0 A}{t} \quad (17)$$

$$Z_p = \frac{1}{C\omega} \quad (18)$$

where  $A$  and  $t$  are the top surface and thickness of the piezoelectric beam respectively. The output voltage measured at the load can be determined using the following formula:

$$V_{out} = \frac{|V_{oc}| R_L}{|Z_p + R_L|} \quad (19)$$

where  $Z_p$  is the piezoelectric impedance and  $R_L$  is the resistance load. From the pacemaker data sheet given by Medtronic (Medtronic 2017), the impedance of a pacemaker varies from 500 to 900  $\Omega$  (Medtronic 2017). The higher impedance offers the shorter live span of the battery. Thus, for the present model, a load impedance of 900  $\Omega$  is used to considered the extreme scenario. The electrical power feed to the load can be written as (Liu et al. 2011a, 2011b):

$$P_{out} = \frac{|V_{oc}|^2 R_L}{2|Z_p + R_L|^2} \quad (20)$$

The maximum power transfer is obtained by matching the impedance of the load and the one of the piezoelectric materials (Andanje, Ikua, and Elbab 2019; Liu et al. 2011a).

## Results and discussion

Two simulations are run using COMSOL Multiphysics software. These are the eigenfrequency study for modal analysis, and time dependent study for stress analysis.

### Beam dimensions

The 2-DOF harvester system is build directly in COMSOL Multiphysics Software (Figure 7). The total length of the system is 26 mm, its width is 11.58 mm and its height is 0.41 mm. The harvester cover a total volume of 0.12  $\text{cm}^3$ . The software's materials library contain the PMMA, Cooper and PZT-5A used for the present system. The parameters obtained from the design process are shown in Table 2.

### Modal analysis

The eigenfrequency study helps to determine the different modes of the system, and the corresponding displacement of the beam. The purpose of this simulation is to determine if the model has the same resonant

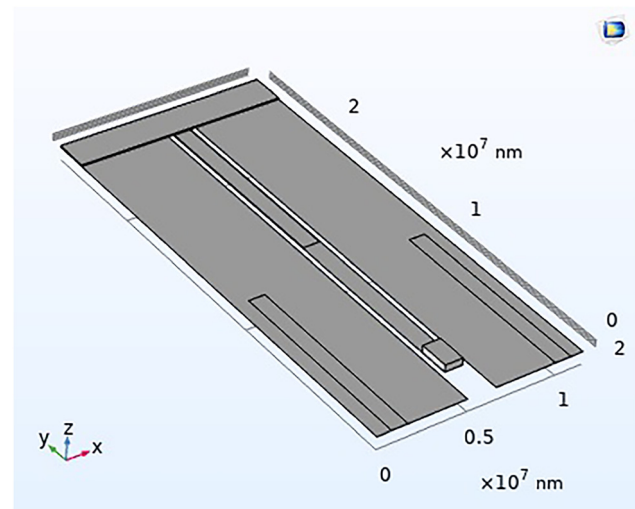


Figure 7: Model 2-DOF.

**Table 2:** 2-DOF systems parameters.

Parameters	Primary beam	Secondary beam
Thickness	10 $\mu\text{m}$	10 $\mu\text{m}$
Length	26 mm	22 mm
Width	$(b_{k1/2})$ 4.79 mm	1 mm
Tip mass	$2 \times 10^{-5}$ g	$6 \times 10^{-6}$ g
Stiffness	$12.06 \times 10^{-5}$	$7.45 \times 10^{-5}$
Length of the piezoelectric beam ( $l_p$ )	11 mm	11 mm
Width of the piezoelectric beam ( $b_p$ )	0.9 mm	0.9 mm
Thickness of the piezoelectric beam ( $t_p$ )	5 $\mu\text{m}$	5 $\mu\text{m}$
Length of tip mass	1.92 mm	1.67
Width of tip mass	11.58 mm	1 mm
Height of tip mass	0.1 mm	0.4 mm

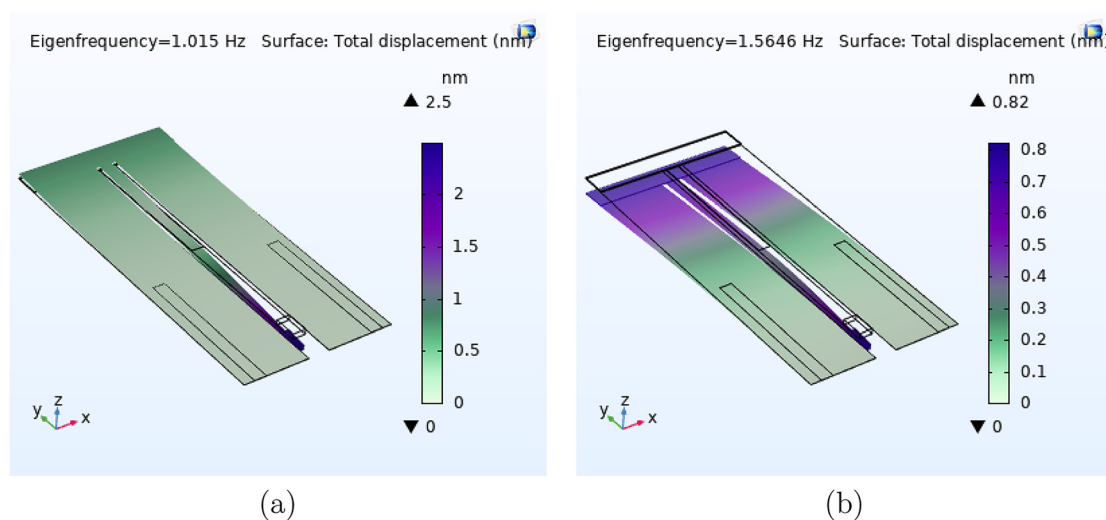
frequencies as set in the design process. The first mode is 1.01 Hz with a total displacement of 2.5 nm, and the second mode is 1.56 Hz with a total displacement of 0.82 nm (Figure 8). The system is behaving as expected with resonant frequencies within the human heartbeat frequencies range. This ensures that the harvester can operate from heartbeat frequencies. At the first frequency, the displacement of the primary beam is very small compared to the one of secondary beam, but at the second frequency, both primary and secondary beams have an important amount of displacement. The results from modal analysis confirm the importance of considering the stiffness of the piezoelectric beam for a micro system design.

## Stress analysis

The stress analysis done in COMSOL provides the value of the stress throughout the piezoelectric beam, represented in Figure 9. At the first frequency, stress in the piezoelectric beams is 2.08 Pa, while it is 22.3 Pa at the second frequency. The stress in the piezoelectric beams is very small. The analytical result of stress in the driving beam using Equation (10), are 2.1 and 7.76 MPa for the primary and secondary beams respectively. The stresses in both the lead (PMMA) and piezoelectric (PZT) beams are under the maximum allowed for the materials.

## Voltage analysis

The system has a total of three piezoelectric beams. The primary beam produces the highest amount of voltage, compared to the secondary beam. The average open-circuit voltage determined using Equation (16) is of 504.66 V (Figure 10(b)), sufficient to power a pacemaker, and 72 times larger than the one obtained after boosting in (Kumar et al. 2018). The impedance of the piezoelectric material is relatively high (Soliman 2009), compared to the 900  $\Omega$  load impedance of the pacemaker. The calculated impedance using Equation (18) is 50.44 M $\Omega$ , about 57.51% of the impedance obtained in (Andanje, Ikua, and Elbab 2019). From the resulted output voltage obtained using Equation (19), two peak voltages are observed at 1.1 and 1.5 Hz (Figure 10(a)). The maximum output voltage of is 0.24 V, obtained at 1.5 Hz.

**Figure 8:** Simulated resonant frequency of the system: (a) first mode; (b) second mode.

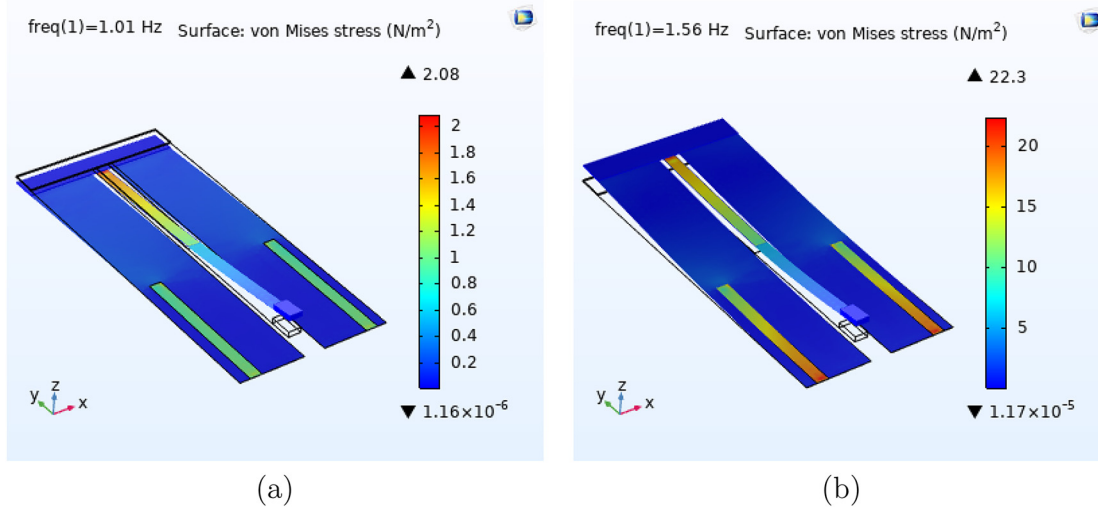


Figure 9: Simulated stress of the system at resonant frequencies: (a) first frequency; (b) second frequency.

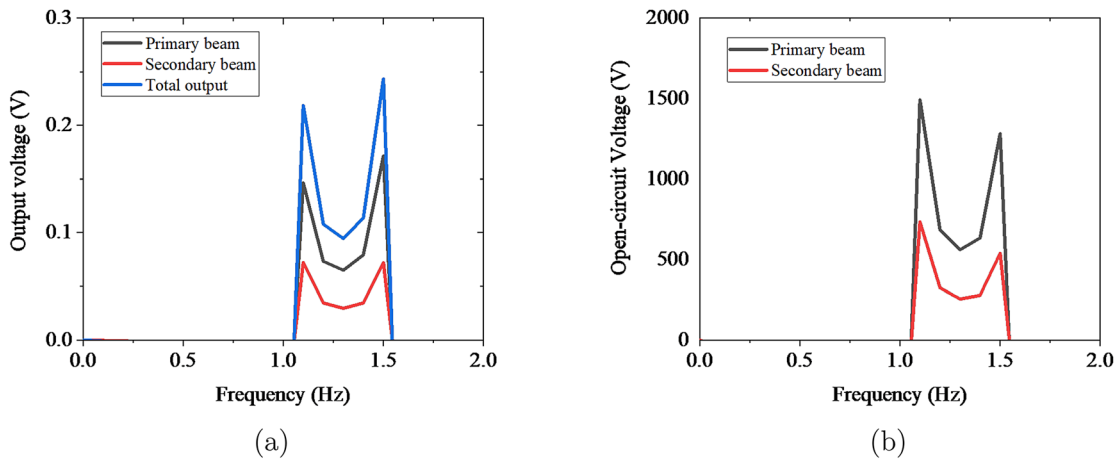


Figure 10: Voltage: (a) output voltage; (b) open-circuit voltage.

## Power analysis

The power shown in Figure 11 is determined considering the scenario where the energy harvester supplies directly the pacemaker, using Equation (20). The figure shows the power output of each beam and the total power output, which is the sum of the two powers. The load impedance is  $900\Omega$ , which is the maximum impedance of a pacemaker (Medtronic 2017). The average output power of  $11.05\ \mu\text{W}$  throughout the frequency range of human heartbeat is obtained by arithmetic mean. Two peak power are observed:  $20.87\ \mu\text{W}$  at 1 Hz, and  $30.97\ \mu\text{W}$  at 1.6 Hz. Modern pacemakers need  $1\ \mu\text{W}$  to operate (Amin Karami and Inman 2012), and the maximum power required is of  $20\ \mu\text{W}$  (Mitcheson et al. 2008). Therefore, the power

produced by the present energy harvester is well adapted for charging and powering a pacemaker. The peak power obtained in the present work is 258–884% higher than the reported work on energy harvester for medical implant application, using blood flow forces and pressure, and the SDOF system configuration (Abdelmageed, El-Bab, and Abouelsoud 2019; Abdelmageed, Fathelbab, and Abouelsoud 2019; Allahverdi 2020). This advantage is mostly due to the 2-DOF system configuration, which offers high power and wide bandwidth compared to the SDOF system (Maamer et al. 2019). The reduction of the battery in size could as well have an impact on its life span. Moreover the integrated harvester will charge it regularly and relay it in case of failure. This could double the working time of pacemakers.

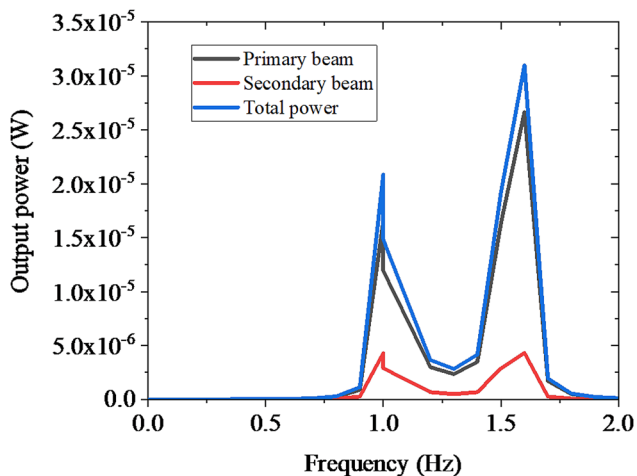


Figure 11: Electrical output power.

## Conclusion

Typical batteries of pacemaker last from 5 to 10 years before it is recharged. There is a real need of increasing the operating time of pacemakers and other medical implant, to reduce the number of surgical interventions on patients. This paper was focused on investigating a 2-DOF piezoelectric energy harvester system for powering a pacemaker, from the human heartbeat frequencies. The very low frequencies and the strict space available in a pacemaker have influence on the design process. The small difference in size between the lead and piezoelectric beam has led to consider the stiffness of both beams to obtain the proper resonant frequencies. When the pacemaker is loaded, the proposed system produces sufficient average power of  $11.05 \mu\text{W}$  throughout the frequency range of 1–1.67 Hz. The harvester produces enough power to supply a pacemaker, and can operate within the range of heartbeat frequencies. This is assumed to extend the life time of pacemaker by 5–10 more years. For further work, it is planned to experimentally validate the proposed device, and provide a mathematical simulation of the number of years the device could add to pacemakers life time. Also, for further investigations, it may be useful to consider stretchable materials in the 2-DOF system configuration to reduce the size of the device or obtain considerable amount of displacement, hence produce higher output power.

**Author contributions:** All the authors have accepted responsibility for the entire content of this submitted manuscript and approved submission.

**Research funding:** The authors would like to thank Pan African University Institute for Basic Sciences Technology

and Innovation (PAUSTI) and Japan International Cooperation Agency (JICA) for their financial support towards this research.

**Conflict of interest statement:** The authors declare no conflicts of interest regarding this article.

## References

- Abdelmageed, M. G., A. M. F. El-Bab, and A. Abouelsoud. 2019. "Design and Simulation of Pulsatile Blood Flow Energy Harvester for Powering Medical Devices." *Microelectronics Journal* 86: 105–13.
- Abdelmageed, M. G., A. M. Fathelbab, and A. Abouelsoud. 2019. "Design and Simulation of an Energy Harvester Utilizes Blood Pressure Variation inside Superior Vena Cava." In *2019 58th Annual Conference of the Society of Instrument and Control Engineers of Japan (SICE)*, 1107–12. IEEE, <https://doi.org/10.23919/sice.2019.8859911>.
- Allahverdi, L. 2020. "Piezoelectric Energy Harvester for Medical Use." PhD diss., California State University, Northridge.
- Alrashdan, M. H. 2020. "Mems Piezoelectric Micro Power Harvester Physical Parameter Optimization, Simulation, and Fabrication for Extremely Low Frequency and Low Vibration Level Applications." *Microelectronics Journal* 104: 104894.
- Amin Karami, M., and D. J. Inman. 2012. "Powering Pacemakers from Heartbeat Vibrations Using Linear and Nonlinear Energy Harvesters." *Applied Physics Letters* 100 (4): 042901.
- Andanje, M. N., B. W. Ikua, and A. M. F. Elbab. 2019. "Piezo-electric Energy Harvesting from Human Motion Based on 2-DOF Vibration Absorber Mode: Design Methodology and Experimental Validation." *International Journal of Mechanical & Mechatronics Engineering IJMME-IJENS* 19 (04).
- Beeby, S., and N. M. White. 2010. *Energy Harvesting for Autonomous Systems*. Artech House.
- Bischur, E., and N. Schwesinger. 2012. Energy Harvesting from Floor Using Organic Piezoelectric Modules. In *2012 Power Engineering and Automation Conference*, 1–4. IEEE, <https://doi.org/10.1109/peam.2012.6612556>.
- Colin, M., S. Basrour, and L. Rufer. 2013. "Design, Fabrication and Characterization of a Very Low Frequency Piezoelectric Energy Harvester Designed for Heart Beat Vibration Scavenging." In *Smart Sensors, Actuators, and MEMS VI*, Vol. 8763, 87631P. International Society for Optics and Photonics.
- Den Hartog, J. P. 1985. *Mechanical Vibrations*. Courier Corporation.
- Gusarov, B. 2015. "Pvdf Piezoelectric Polymers: Characterization and Application to Thermal Energy Harvesting." PhD diss., Université Grenoble Alpes.
- Ju, S., S. H. Chae, Y. Choi, S. Lee, H. W. Lee, and C.-H. Ji. 2013. "A Low Frequency Vibration Energy Harvester Using Magnetoelectric Laminate Composite." *Smart Materials and Structures* 22 (11): 115037.
- Kaysons. 2018. *Physical Properties of Acrylic Sheets*. Akrylik Furniture & Accessories.
- Kazmierski, T. J., and S. Beeby. 2014. *Energy Harvesting Systems*. Springer.
- Kuan, J. 2017. *What is the Frequency of Human Heart in Hz*. Also available at <https://www.quora.com/What-is-the-frequency-of-human-heart-in-Hz>.

- Kumar, A., R. Kiran, S. Kumar, V. S. Chauhan, R. Kumar, and R. Vaish. 2018. "A Comparative Numerical Study on Piezoelectric Energy Harvester for Self-Powered Pacemaker Application." *Global Challenges* 2 (1): 1700084.
- Liu, H., C. J. Tay, C. Quan, T. Kobayashi, and C. Lee. 2011a. "Piezoelectric Mems Energy Harvester for Low-Frequency Vibrations with Wideband Operation Range and Steadily Increased Output Power." *Journal of Microelectromechanical Systems* 20 (5): 1131–42.
- Liu, H., C. J. Tay, C. Quan, T. Kobayashi, and C. Lee. 2011b. "A Scrape-Through Piezoelectric Mems Energy Harvester with Frequency Broadband and Up-Conversion Behaviors." *Microsystem Technologies* 17 (12): 1747–54.
- Maamer, B., A. Boughamoura, A. M. F. El-Bab, L. A. Francis, and F. Tounsi. 2019. "A Review on Design Improvements and Techniques for Mechanical Energy Harvesting Using Piezoelectric and Electromagnetic Schemes." *Energy Conversion and Management* 199, <https://doi.org/10.1016/j.enconman.2019.111973>.
- Magdy, M. M., A. M. F. El-Bab, and S. F. Assal. 2014. "Design Methodology of a Micro-scale 2-DOF Energy Harvesting Device for Low Frequency and Wide Bandwidth." *Journal of Sensor Technology* 2014, <https://doi.org/10.4236/jst.2014.42005>.
- Magdy, M. M., N. A. Mansour, A. M. F. El-Bab, and S. F. Assal. 2014. "Human Motion Spectrum-Based 2-DOF Energy Harvesting Device: Design Methodology and Experimental Validation." *Procedia Engineering* 87: 1218–21.
- Medtronic. 2017. *Azure xt dr mri surescan: Model w2dr01*.
- Medtronic. 2020. *Pacemakers*. Also available at <https://www.medtronic.com/us-en/patients/treatments-therapies/pacemakers.html>.
- Mitcheson, P. D., E. M. Yeatman, G. K. Rao, A. S. Holmes, and T. C. Green. 2008. "Energy Harvesting from Human and Machine Motion for Wireless Electronic Devices." *Proceedings of the IEEE* 96 (9): 1457–86.
- Mokhtari, F., G. M. Spinks, S. Sayyar, Z. Cheng, A. Ruhparwar, and J. Foroughi. 2021. "Highly Stretchable Self-Powered Wearable Electrical Energy Generator and Sensors." *Advanced Materials Technologies* 6 (2): 2000841.
- Nia, E. M., N. A. W. A. Zawawi, and B. S. M. Singh. 2017. "A Review of Walking Energy Harvesting Using Piezoelectric Materials." In *IOP Conference Series: Materials Science and Engineering*, Vol. 291, 012026. IOP Publishing.
- Panchenko, I., N. Shandyba, A. Ballouk, D. Rodrigues, A. Kolomiitsev, and O. Ageev. 2020. "Investigation of the Influence of the Geometric Parameters of Afm Cantilevers on the Resonant Frequency of Their Oscillations." In *Journal of Physics: Conference Series*, Vol. 1695, 012182. IOP Publishing.
- Renaud, M., P. Fiorini, R. van Schaijk, and C. Van Hoof. 2009. "Harvesting Energy from the Motion of Human Limbs: The Design and Analysis of an Impact-Based Piezoelectric Generator." *Smart Materials and Structures* 18 (3): 035001.
- Rob Carter, R. K. 2021. *Introduction to Piezoelectric Transducers*. Also available at <https://info.piezo.com/hubfs/Data-Sheets/piezo-material-properties-data-sheet-20201112.pdf>.
- Roundy, S. J. 2003. "Energy Scavenging for Wireless Sensor Nodes with a Focus on Vibration to Electricity Conversion." PhD diss., University of California, Berkeley, CA.
- Sezer, N., and M. Koç. 2020. "A Comprehensive Review on the State-of-the-Art of Piezoelectric Energy Harvesting." *Nano Energy*: 105–567.
- Soliman, Mostafa. 2009. "Wideband Micro-power Generators for Vibration Energy Harvesting." PhD thesis, Ontario, University of Waterloo.
- Thomson, W. 1996. *Theory of Vibration with Applications*. CRC Press.
- Wang, C., S.-K. Lai, J.-M. Wang, J.-J. Feng, and Y.-Q. Ni. 2021. "An Ultra-Low-Frequency, Broadband and Multi-Stable Tri-hybrid Energy Harvester for Enabling the Next-Generation Sustainable Power." *Applied Energy* 291: 116825.
- Wu, Y., J. Qiu, S. Zhou, H. Ji, Y. Chen, and S. Li. 2018. "A Piezoelectric Spring Pendulum Oscillator Used for Multi-Directional and Ultra-Low Frequency Vibration Energy Harvesting." *Applied Energy* 231: 600–14.
- Xu, Z., C. Jin, A. Cabe, D. Escobedo, N. Hao, I. Trase, A. B. Closson, L. Dong, Y. Nie, and J. Elliott. 2020. "Flexible Energy Harvester on a Pacemaker Lead Using Multibeam Piezoelectric Composite Thin Films." *ACS Applied Materials & Interfaces* 12 (30): 34170–9.
- Zayed, A. A., S. F. Assal, K. Nakano, T. Kaizuka, and A. M. Fath El-Bab. 2019. "Design Procedure and Experimental Verification of a Broadband Quad-Stable 2-DOF Vibration Energy Harvester." *Sensors* 19 (13): 2893.
- Zhou, D., N. Wang, T. Yang, L. Wang, X. Cao, and Z. L. Wang. 2020. "A Piezoelectric Nano-Generator Promotes Highly Stretchable and Self-Chargeable Supercapacitors." *Materials Horizons* 7 (8): 2158–67.
- Zhu, D., and S. Beeby. 2011. "Kinetic Energy Harvesting." In *Energy Harvesting Systems*, edited by T. J. Kaźmierski T., and S. Beeby, 1–77. New York: Springer.